

A Study of Longwave Radiation Codes for Climate Studies: Validation with Observations and Tests in General Circulation Models—an Update

R. G. Ellingson and F. Baer
 Department of Meteorology
 University of Maryland
 College Park, MD 20742

Introduction

Research by the U.S. Department of Energy (DOE) has shown that cloud radiative feedback is the single most important effect determining the magnitude of possible climatic responses to human activity. However, these effects are still not known at the levels needed for climate prediction. Consequently, DOE has launched a major initiative—the Atmospheric Radiation Measurement (ARM) Program—directed at improving the parameterization of the physics governing cloud and radiative processes in general circulation models (GCMs).

One specific goal of ARM is to improve the treatment of radiative transfer in GCMs under clear-sky, general overcast, and broken cloud conditions. In 1990, we proposed to contribute to this goal by attacking major problems connected with one of the dominant radiation components of the problem—longwave radiation. In particular, our long-term research goals are to

- develop for use in GCMs an optimum longwave radiation model that has been calibrated with state-of-the-art observations
- assess the impact of the longwave radiative forcing in a GCM
- determine the sensitivity of a GCM to the radiative model used in it
- determine how the longwave radiative forcing contributes relatively when compared with shortwave radiative forcing, sensible heating, thermal advection and expansion.

Our approach to developing the radiation model is to test existing models in an iterative, predictive fashion. We plan

to compare calculations from a set of models with operationally observed data. The differences we find will lead to the development of new models to be tested with new data. Similarly, our GCM studies will use existing GCMs to study the radiation sensitivity problem. We anticipate that the outcome of this approach will provide both a better longwave radiative forcing algorithm and a better understanding of how longwave radiative forcing influences the equilibrium climate of the atmosphere.

This report summarizes the research results obtained since the last ARM Science Team meeting under the categories of Radiation Model Testing Activities and General Circulation Model Testing Activities. Additional details may be obtained from the authors.

Radiation Model Testing Activities

Longwave radiation quantities—radiances, fluxes and heating rates—are usually calculated in GCMs as the cloud amount weighted average of the values for clear and homogeneous cloud conditions. For example, the downward flux at the surface, F_{\downarrow} , may be written as

$$F_{\downarrow} = (1 - N^*) F_{o\downarrow} + N^* F_{c\downarrow} \quad (1)$$

where $F_{o\downarrow}$ is the flux that would occur if the sky were clear with the observed, non-cloud radiative properties, $F_{c\downarrow}$ is the flux that would occur if the sky were completely covered by a single plane-parallel cloud layer of uniform

optical properties, and N^* is the “effective” fraction of the sky covered by plane-parallel clouds. The equation is deceptively simple, but there are significant problems associated with the calculation of $F_{o\downarrow}$, $F_{c\downarrow}$, and N^* .

Our research program is directed at problems associated with each of the three terms. We have made significant progress in determining the

- ability of line-by-line radiation models to calculate the F_{\downarrow} at the surface
- uncertainties in calculating the downwelling radiance and flux at the surface associated with the use of different profiling techniques
- variability among calculations from radiation codes from different climate models and their differences relative to clear-sky radiance and flux observations
- uncertainties associated with estimating N^* from surface longwave flux observations
- sensitivity of calculations to different formulations of finite-sized clouds.

These topics are discussed below.

Clear-Sky Studies

We have begun to compare clear-sky spectra of the downwelling radiance at the surface observed during SPECTRE (Spectral Radiance Experiment) with FASCOD3P and with narrow- and broad-band radiation models. Examples of such spectra are shown in Figure 1, and the mean difference between the observed and FASCOD3P calculated radiance for 26 different spectra is shown in Figure 2a. The FASCOD3P line-by-line model calculations were performed using near simultaneous radiosonde temperature and Raman water vapor profiles with surface-based trace gas data and the 1992 line compilation as input.

In general, the line-by-line model captures most of the features in the observed clear-sky spectra. The model tends to underestimate the observed radiance in the window region between 800 to 1000 cm^{-1} and to overestimate it in portions of the 1200 to 1400 cm^{-1} region. However, we are not yet in the position to make firm conclusions concerning the spectral and absolute character of the differences because the final instrument calibration

is not yet complete. Nevertheless, the differences in many locations is of the order or smaller than the estimated absolute accuracy of the observations (~1% full scale of Figure 1).

Our sensitivity analysis of the radiation calculations shows that with the expected 5% humidity and 0.5 K temperature accuracies, the uncertainties in the calculations due to errors in the meteorological data should be kept below about 8% in the regions of relatively strong lines and below about 5% in weakly absorbing regions. In the transparent region of the spectrum from 800 to 1000 cm^{-1} , narrow-band model radiances calculated using the Roberts et al. (1976) continuum and those using the more recent continuum of Clough et al. (1992) used in FASCOD differ by about 30%, and they show a particular spectral signal.

The differences between the observed and calculated spectra in the 800 to 1000 cm^{-1} region for the highest water vapor amounts seen during SPECTRE (~2 cm precipitable H_2O) show that the FASCOD continuum yields better results than Roberts et al. The data from the drier cases cannot be used to support this conclusion at this time because the absolute error of the observations is larger than the radiance in the more transparent regions of the 800 to 1000 cm^{-1} region. However, as the instrument calibrations are completed, it will be possible to use the high relative accuracy to check the spectral signatures of the differences and to put error bars on them.

We recently completed 26 sets of comparisons of Atmospheric Emitted Radiance Interferometer (AERI) observations with FASCOD calculations using near simultaneous water vapor profiles from radiosondes, Westwater’s microwave radiometer, and Melfi’s Raman lidar. The spectral distribution of the RMS differences (Figure 2b) shows that the Raman data yield a more consistent spectral pattern of differences between observations and calculations than occurs when the radiosonde or microwave data are used in the calculations. As the calibration of the AERI is finalized, it will be possible to use the high relative accuracy of the observations to check the spectral signatures of the differences between observations and calculations and to put better error bars on the absolute differences. The improved calibration data and Cloud and Radiation Testbed (CART) site observations over larger water vapor amounts should allow more stringent tests of the continuum formulations than possible heretofore, particularly if a Raman lidar is used for profiling water vapor.

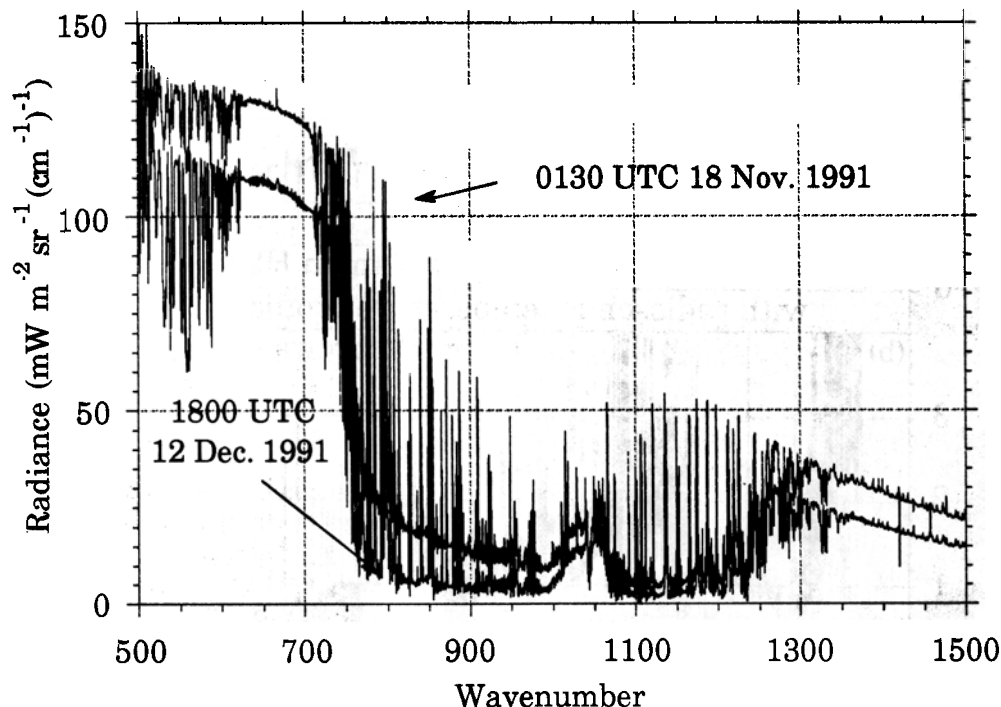


Figure 1. Examples of AERI spectra from SPECTRE.

Climate modelers are also anxious to test the ability of their radiation codes to calculate the total downward flux. The radiance observations can be integrated over the observed portion of the spectrum to yield estimates of the flux uncertainty if one assumes the angular variation is known. Note that for a given plane parallel, horizontally homogeneous atmosphere, the downward flux may be related to the vertically downward radiance $I(0)$ as $F_{\downarrow} = \pi I(0)L$ where

$$L = \int_0^1 \frac{I(\mu)}{I(0)} \mu d\mu \quad (2)$$

$\mu = \cos \theta$, and θ is the local zenith angle.

To first order, we assume L to be a property of the temperature and water vapor distributions and not of the ability to calculate I . Thus, the soundings may be used with FASCOD to calculate L , and the uncertainty in F_{\downarrow} for the observed spectral interval is given approximately as

$$\delta F_{\downarrow} = \pi L (I_{\text{obs}}(0) - I_{\text{cal}}(0)) \quad (3)$$

We are in the process of calculating L from (2) using FASCOD3P for the SPECTRE soundings; we will also do this for CART data as they become available. In the interim, we have estimated δF using the diffusivity approximation as calculated by MODTRAN. When integrated over the 550 to 1500 cm^{-1} interval, the comparisons indicate the mean (observed - calculated) flux uncertainty of the FASCOD calculations to be 0.4 ± 0.2 , 0.5 ± 0.5 , and $1.2 \pm 0.3 \text{ W}\cdot\text{m}^{-2}$, depending upon the use of Raman, radiosonde or microwave water vapor profiles, respectively. For individual soundings, the results show that the downward flux for this interval may be calculated to within about $\pm 2 \text{ W}\cdot\text{m}^{-2}$ for any of the sounding types.

The data do not allow us to estimate the uncertainties in the 0 to 550 cm^{-1} region. However, since this portion of the spectrum is nearly opaque for the conditions we observed during SPECTRE, the uncertainties in calculating the

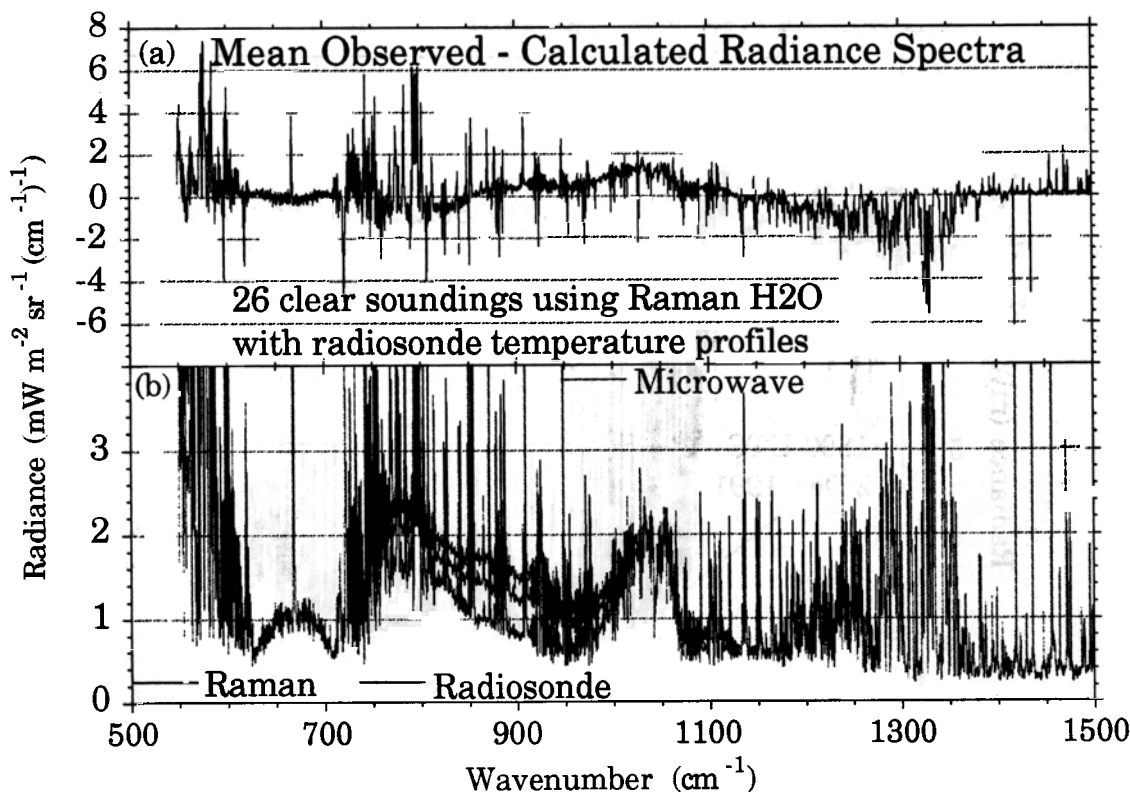


Figure 2. Mean (a) and RMS (b) AERI observed minus FASCOD3P calculated radiance spectra from SPECTRE.

downward flux at the surface from this portion of the spectrum are relatively small. Thus, we plan to estimate the flux for homogeneous clear and cloudy conditions with model calculations for the 0 to 550 cm^{-1} region and with (1) for the 550 to 3000 cm^{-1} region and compare the results with observations from the pyrometers located at the CART and SPECTRE sites. Since the uncertainties in the interferometer data are smaller than those associated with the pyrometers, we believe that the interferometer-based flux data will serve as a baseline calibration of the pyrometers for homogeneous clear or cloudy conditions.

A disturbing trend of the differences between the AERI “observed” and calculated fluxes is that differences become more negative as the total precipitable water (PW) increases, independent of the source of water vapor data. The calculated flux (integrated radiance for the 550 to 1500 cm^{-1} region) is greater than that observed for six of the nine cases with PW > 1.4 cm. These differences appear to be

correlated primarily with PW in the 1100 -1200 cm^{-1} region and with surface temperature in the 725 -850 cm^{-1} region. These differences hint at potential problems in the continuum formulation—temperature dependence in the self-broadened term and the magnitude of the continuum coefficients in the foreign broadened regions. Clough et al. (1992) show results consistent with ours in the higher wavenumber regions, although the amount of water in the atmosphere during those observations was considerably less than the amount we found during SPECTRE. We will have to closely examine CART observations at the Southern Great Plains (SGP) and tropical Western Pacific (TWP) sites at higher water vapor amounts and temperatures to see if these differences continue.

During the past 12 months we began preparing for operational testing of a variety of narrow- and broad-band models with CART observations by intercomparing calculations with spectrally integrated AERI observations

from SPECTRE. The suite of models includes several used in GCMs (including GLA, CCM1, CCC, NMC, RPN and ECMWF) and several detailed models (e.g., the Air Force Geophysics Laboratory's MODTRAN and LOWTRAN7, and Ellingson's narrow-band model). We modified several of the GCM-type models to calculate radiance, rather than flux. Furthermore, we grouped output into common spectral intervals for comparison purposes, although this cannot be done for all models because not all calculate in the same spectral interval and not all can be modified to give results in those spectral intervals sensed by the AERI.

We started our study by examining the more transparent 800 - 1200 cm^{-1} region since the Intercomparison of Radiative Codes in Climate Models (ICRCCM) Program indicated that uncertainties associated with the water vapor continuum make this the most suspect portion of the spectrum. Figure 3 shows an intercomparison of some of the statistical properties of the various model calculations and AERI observations in the 800 - 1200 cm^{-1} region using the 26 clear-sky radiosonde temperature and water vapor profiles noted above as input.

Some large differences occur in the medians, but these appear to be largely systematic for all models, as the

fractional variance of the AERI observations explained by the different models is about the same. The latter result may largely be the result of the small range of PW sensed during SPECTRE. Clearly, some of the models have deficient parameterizations of the water vapor continuum, and these will have to be changed in order for the models to yield correct radiances and fluxes over the full range of atmospheric conditions. Note also that the correlations decreased for each of the models when the 9.6- μm ozone band was included in the comparisons (Figure 3b). We believe this to be a result of a few poor ozonesonde profiles in the sample, but this will have to be studied in greater detail.

Dr. John DeLuisi of the National Oceanic and Atmospheric Administration (NOAA) carried out a pyrgeometer intercomparison during SPECTRE. The data from that study allow the possibility of intercomparing model flux calculations with observations; they also allow the possibility of calibrating the pyrgeometers with the interferometer. Shown in Figure 4 is an intercomparison of fluxes calculated by the NMC radiation model and those observed by a pyrgeometer at the launch time of the 26 soundings discussed above. No attempt was made to ensure that the sky was *completely* clear during these soundings, although clear sky conditions at the zenith were observed.

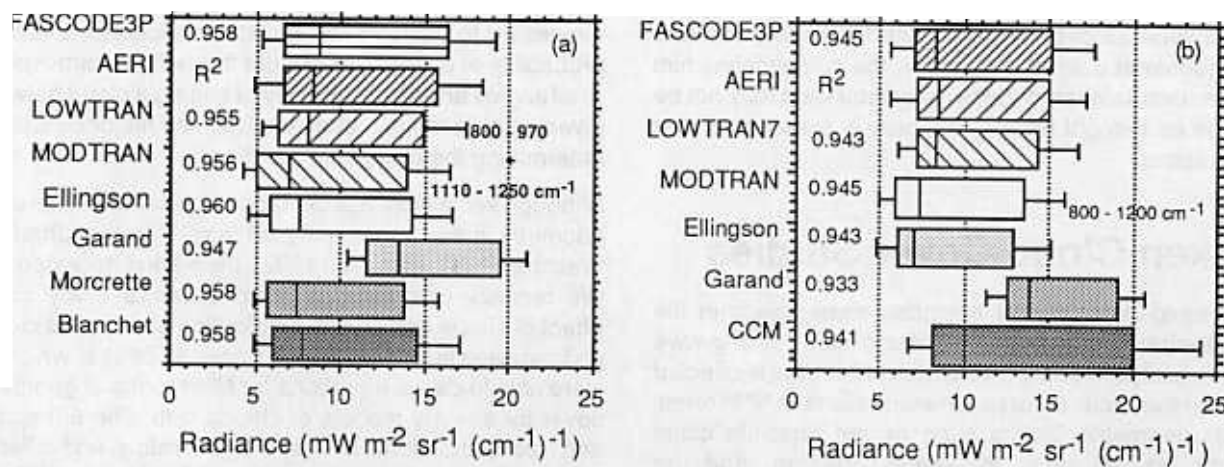


Figure 3. Distributions of vertically downwelling radiance at the surface for 26 clear-sky cases as calculated by several different models and observed by the AERI during SPECTRE. The vertical lines in the boxes show the median values. The edges of the boxes mark the limits of $\pm 25\%$ of the population, and the lines extending from the boxes mark the minimum and maximum values. The fraction of the AERI variance explained by each model is shown in the column marked R^2 .

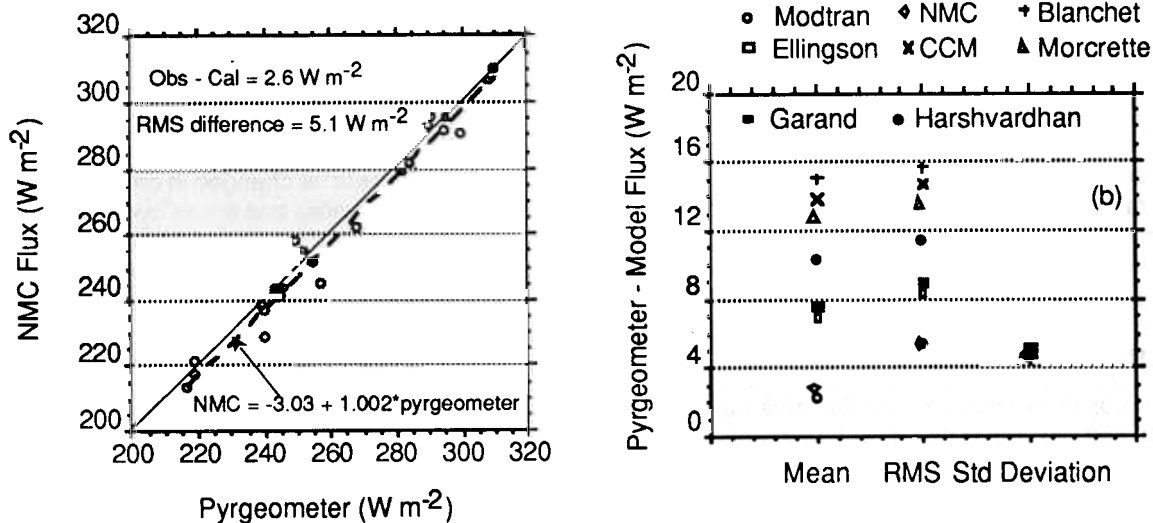


Figure 4. Comparisons of model calculated with pyrgeometer observed clear-sky downward fluxes at the surface during SPECTRE. (a) NMC model; (b) Statistics from other models.

Overall, the results are quite impressive. For this set, the NMC model underestimates the observed fluxes by about $3 \text{ W}\cdot\text{m}^{-2}$ in the mean, and the RMS difference is about $6 \text{ W}\cdot\text{m}^{-2}$. The other models have somewhat greater biases, but all models have about the same RMS error when the biases are removed—about $6 \text{ W}\cdot\text{m}^{-2}$. These comparisons are very consistent with the model-interferometer comparisons. Since the nominal accuracy usually ascribed to pyrgeometer data is about $\pm 5\%$, the comparisons hint that the uncertainties in the pyrgeometer data may not be as large as thought when great care is exercised in the observations.

Broken Cloud Cover Studies

Since liquid-water clouds are often nearly black in the thermal infrared, cloud geometry dominates the longwave broken cloud problem. Our research in this area is directed at testing the accuracy of parameterizations of N^* in terms of bulk geometric factors such as the absolute cloud amount, aspect ratio, thickness, spacing, and the distribution of clouds on the horizontal plane. However, a number of difficulties are associated with research on this problem, including

- Finite-size cloud effects on $F_{o\downarrow}$ at the surface are generally within the 5% accuracy of pyrgeometer observations.
- There are no standard methods for estimating the required cloud properties.

If clouds were black and randomly distributed, the quantities necessary to perform the radiation calculations are the probability of a clear line of sight through the atmosphere at all angles and the probability of seeing a cloud between given altitude regions at all angles. The major difficulty is determining the probability functions.

Although some work has been done on the effects of cloud geometry in the thermal infrared (e.g., Harshvardhan and Weinman 1982; Ellingson 1982), the work is not extensive. We recently completed a comprehensive study of the effect of shape and spatial distribution of cumulus clouds on longwave flux (Killen and Ellingson 1993) in which we were able to derive equations for N^* in terms of geometric cover for several models of clouds with different spatial and size distributions, different aspect ratios, and different shapes. Overall, the study has found that N^* is sensitive to cloud shape and aspect ratio but is insensitive to the cloud spatial distribution or distribution of cloud area. This is

because the cloud distribution must be normalized to geometric cover, and this is the dominant factor. N^* is also very sensitive to the thermal gradient between the cloud top and base.

Our research on using observations for testing models of N^* is following two different approaches. One approach will determine N^* from a combination of flux and radiance observations and/or calculations using a variation of the spatial correlation technique used for determining cloud amount from satellite data. We will then compare the estimated N^* with those calculated by the theoretical models using data from the three-dimensional mapping network.

The uncertainty in estimating N^* depends primarily on the uncertainty of the measured flux components [i.e., F , F_o and F_c in (1)]. Assuming the error of the flux components to be random with equal standard deviation σ_f , the standard deviation of the uncertainty of N^* , $\sigma_{\delta N^*}$, for one cloud layer may be written as

$$\sigma_{\delta N^*} = \frac{\sigma_f \sqrt{2}}{F_o - F_c} \sqrt{[1 + N^*(N^* - 1)]} \quad (4)$$

Note that F_o depends upon the temperature and water vapor distributions, and F_c depends additionally on the altitude of the cloud base. We have calculated $\sigma_{\delta N^*}$ for the five McClatchey (1971) soundings and cloud base altitudes

ranging from 0.5 to 3 km. The results for $\sigma_f = 5 \text{ W}\cdot\text{m}^{-2}$ are shown in Figure 5a. The variation of N^* with N for different cloud shapes is shown in Figure 5b for comparative purposes.

In general, the results show that the uncertainty of individual estimates of N^* is of the order of 0.1 when the flux observations have uncertainties of the order of $5 \text{ W}\cdot\text{m}^{-2}$. This magnitude of uncertainty will not allow us to distinguish between the formulations for random distributions of cubes or cylinders at $N = 0.4$, for example. However, it will allow us to validate the general shape of the form of the variation of N^* with N for different size clouds.

Our second approach to estimating N^* from observations is to use scanning lidars, cloud radars, and cloud imagery to develop empirical probability statistics. This is similar to performing Monte Carlo simulations on a computer, but here the atmospheric physics change the cloud parameters and a lidar tracks the photons. The observed probability statistics will be compared with those calculated from simple geometrical considerations.

Dr. Ezra Takara, an expert in Monte Carlo radiation calculations for engineering applications, has recently joined our group and is working with us to develop our ability to interpret the anticipated cloud observations. In particular, Dr. Takara will be generating clear and cloudy line-of-sight probability statistics for clouds of mixed

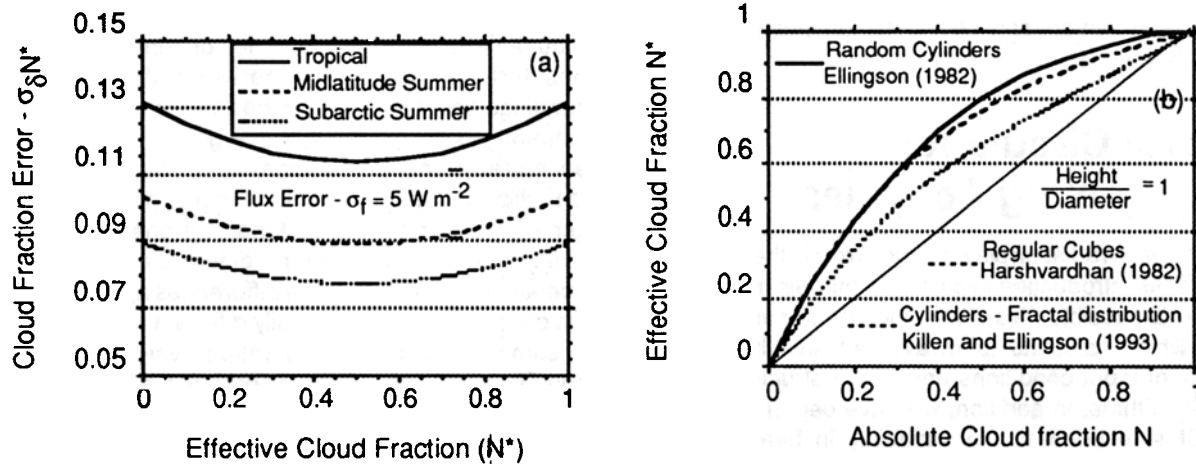


Figure 5. (a) Effects of flux estimation error on estimates of N^* . (b) Distribution of N^* with N for different shapes and distributions.

geometry and will be calculating fluxes which include the effects of multiple scattering. These calculations are necessary because clouds are not completely opaque in the IR, and because our analytic emission studies give results for average type of effects. The Monte Carlo simulations should allow us to determine the manner of interpreting the cloud imagery, radar and lidar observations when they become available. Such data when combined with the approach using the flux data should allow us to more precisely determine the manner by which the effective cloud fraction varies with cloud parameters.

As information concerning the cloud and aerosol properties becomes more readily predictable in GCMs, it will be necessary for the longwave radiation models to include the effects of multiple scattering as well as thermal emission. Including multiple scattering effects is relatively straightforward if one uses a k-distribution technique. However, there are potential drawbacks to this technique as concerns the number of k's and the temperature and pressure scaling. An alternative approach is to use the effective beam-length as done in many heat transfer studies (e.g., Yuen 1990; Yuen and Takara 1990). This type of approach was discussed by Taylor and McCleese (1976) with application to some remote sensing problems, but its application to climate problems has not been extensive. The advantage of the approach is that current techniques for calculating longwave transfer may be used by modifying the absorber amount and/or effective pressure. Ms. Anne Costolanski, a Ph.D. student in our group, is studying the feasibility of such techniques as part of her dissertation research, and we plan to continue this during the next few years.

General Circulation Model Testing Activities

Since longwave radiation plays a crucial role in the evolution of climate, its introduction into climate models must be as accurate as possible. We have studied the sensitivity of models which calculate longwave radiative heating to variability of input conditions and to the structure of the model algorithms. In addition, we have begun to assess how GCMs respond to the variability in heating rates provided by the longwave radiation algorithms.

To understand the sensitivity of heating rates to longwave radiation model algorithms (LWRMs), we have

intercompared seven such models—most of which are currently used in a unique GCM. The institutions involved are CCC (Canada), ECMWF (United Kingdom), National Center for Atmospheric Research (NCAR) (United States), Colorado State University (CSU) (United States), UMCP (United States), RPN (Canada), and NMC (United States). Input data to each of these models include vertical soundings of temperature, water vapor mixing ratio, ozone, and clouds when applicable (as of this date we have tested the models primarily under clear sky conditions). To establish systematic tests of the selected algorithms, we have prepared several data sets. For reference to previous studies, we have used the standard McClatchey (1971) soundings. For more careful analyses, we have compiled 100 soundings for each of four regional/seasonal domains based on a large data set presented by Phillips et al. (1988). These soundings allow us to look at mean profiles as well as standard deviations from those means. The four Phillips data sets show significant variability in the temperature and moisture profiles, both among themselves in the mean and in the standard deviations within each set.

The heating rates produced by the algorithms for the available data sets show significant variability, frequently varying in excess of 0.5 K/day over a large range in the vertical. If one uses more levels in the vertical, the profiles are smoother, but the general shape is reasonably preserved when a 30-level calculation is compared with an 18-level one.

We discuss results with 18 levels because it is in the range of current models, in particular, the NMC model which produces weather forecasts. The horizontal profiles show considerable differences between the McClatchey soundings and the means of the Phillips soundings when comparing over seasons and regions. Analysis of the heating rates and their standard deviations produced by the Phillips soundings shows pronounced variability within each of the four data sets. Finally, if one compares the heating rates produced by the different algorithms using correlation coefficients, large differences appear. One can thus conclude that substantially different heating rates for the same sounding data are made available to a GCM, depending only on which algorithm the GCM applies. Since this conclusion is based on clear sky analysis, one can speculate that cloudy sky calculations would exacerbate this situation.

Does this sensitivity play a role when the chosen LWRM is introduced into a GCM? A systematic test to identify such

sensitivity would require the introduction of various LWRMs into the same GCM and integrations to be performed for a variety of climate scenarios. We plan an experiment of this type but as a preliminary study, we used archives of climate runs and compared the data derived therefrom to give some indication of sensitivity. Currently available to us are extended climate runs with the NCAR CCM1 and CCM2. The archives include profiles of output of the LWRM heating rates in the model over the entire globe and at frequent intervals during the integration. We have analyzed heating rates for those models for a January-February period taken from the archives for the CCM1 (R15), CCM1 (T42), and CCM2 (T42). For these three models, the data are taken for the same time period. We have analyzed the data over the two months and calculated standard deviations from the means. The data are presented on each model level and in terms of the expansion coefficients of the spectral components, effectively yielding the amplitudes of the heating rates in terms of spatial scales. To compare the vertical resolution, vertical means were also calculated (external mode), and deviations from those means were evaluated (internal mode).

The results of these calculations, although striking, were not unexpected. Most pronounced was the difference in the horizontal and vertical distribution of heating rates produced by the R15 and T42 models of the CCM1. We can fairly report that these heating rates were completely different, although the total amplitude was in the same range. This was true for all spatial scales except the overall global value with height and the vertical distribution in the mean zonal field. Moreover, the amplitude as a function of meridional scale did not decay with decreasing scale in the R15 model, subjecting that model to potentially serious nonlinear computational errors. The heating rates generated by the T42 model did decay with decreasing scale.

To a limited extent, we were able to test the interannual variations relative to the intraannual variations by analyzing a second annual season (a different January-February archive) for the CCM1. If we define the difference in the winter mean of the two annual seasons as the interannual variation and compare it with the standard deviation of heating rates for one of the winter seasons, we find that the intraannual variation (standard deviation) is considerably larger than the interannual variation. We can thus feel more comfortable in an analysis of one of the annual winter periods.

Analysis of the January-February period taken from the CCM2 (T42) shows distributions which differ to some extent from the CCM1 (T42) but have more similarities than the comparison of the CCM1 runs based on truncation. Nevertheless, changes in the CCM2 result in heating rates which decrease more rapidly with decreasing scale when compared with the CCM1.

We currently are setting up a plan to test various LWRMs in a specific GCM, hopefully, one available at Lawrence Livermore National Laboratory. Concurrently, we are collecting heating rate data generated from several models which have produced data for the Atmospheric Model Intercomparison Project (AMIP) and plan to intercompare those data to assess model sensitivity.

References

- Clough, S. A., M. J. Iacono, and J.-L. Moncet. 1992. Line-by-line calculations of atmospheric fluxes and cooling rates: Application to water vapor. *J. Geophys. Res.* **97**:15761-15785.
- Ellingson, R. G. 1982. On the effects of cumulus dimensions on longwave irradiance and heating rates. *J. Atmos. Sci.* **39**:886-896.
- Harshvardhan, and J. A. Weinman. 1982. Infrared radiative transfer through a regular array of cuboidal clouds. *J. Atmos. Sci.* **39**:431-439.
- Killen, R. M., and R. G. Ellingson. 1993. The effect of shape and spatial distribution of cumulus clouds on longwave irradiance. Submitted to *J. Atmos. Sci.* April 1993.
- Lacis, A. A., and V. Oinas. 1991. A description of the correlated k-distribution method for determining nongray gaseous absorption, thermal emission, and multiple scattering in vertically inhomogeneous atmospheres. *J. Geophys. Res.* **96**:9027-9074.
- McClatchey, R. A., R. W. Fenn, J.E.A. Selby, F. E. Volz, and J. S. Garing. 1971. *Optical Properties of the Atmosphere*. Rep. AFCL-71-0279, Air Force Cambridge Res. Lab., Bedford, Massachusetts.
- Phillips, N., J. Susskind, and L. McMillin. 1988. Results of a joint NOAA/NASA sounder simulation study. *J. Atmos. Ocean Tech.* **5**:44-56.

Roberts, R. E., J.E.A. Selby, and L. M. Biberman. 1976. Infrared continuum absorption by water vapor in the 8-12 μm window. *Appl. Opt.* **15**:2085-2090.

Taylor, F. W., and D. J. McClesse. 1976. Multiple scattering in broad spectral bands. *Radiation in the Atmosphere*, H.-J. Bolle, ed., p. 271-273. Science Press, Princeton, New Jersey.

Yuen, W. W. 1990. Development of a network analogy and evaluation of mean beam lengths for multi-dimensional absorbing/isotropically-scattering media. *AMSE J. Heat Transfer* **112**:408-414.

Yuen, W. W., and E. Takara. 1990. Development of a generalized zonal method for the analysis of radiative heat transfer in absorbing and anisotropically scattering media. *Numerical Heat Transfer*, eds. K. Vafai and J.L.S. Chen, ASME HTD **130**:123-132.